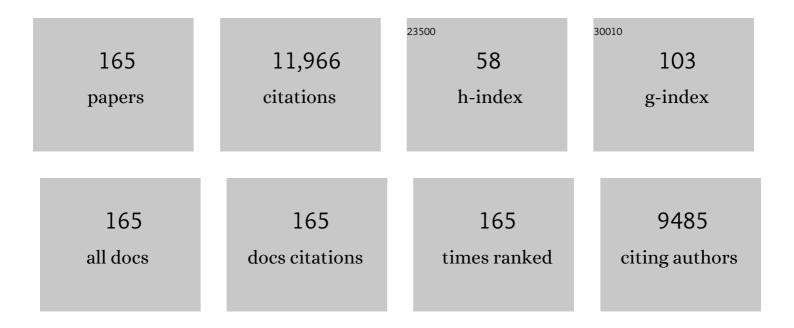
Wang Yimin

List of Publications by Year in descending order

Source: https://exaly.com/author-pdf/7354846/publications.pdf Version: 2024-02-01



MANC YIMIN

#	Article	IF	CITATIONS
1	Manipulation of Persistent Free Radicals in Biochar To Activate Persulfate for Contaminant Degradation. Environmental Science & Technology, 2015, 49, 5645-5653.	4.6	684
2	Activation of Persulfate by Quinones: Free Radical Reactions and Implication for the Degradation of PCBs. Environmental Science & amp; Technology, 2013, 47, 4605-4611.	4.6	673
3	Photocatalytic degradation of tetracycline in aqueous solution by nanosized TiO2. Chemosphere, 2013, 92, 925-932.	4.2	543
4	Superoxide radical driving the activation of persulfate by magnetite nanoparticles: Implications for the degradation of PCBs. Applied Catalysis B: Environmental, 2013, 129, 325-332.	10.8	420
5	Sulfate radical-based degradation of polychlorinated biphenyls: Effects of chloride ion and reaction kinetics. Journal of Hazardous Materials, 2012, 227-228, 394-401.	6.5	356
6	Transport of Biochar Particles in Saturated Granular Media: Effects of Pyrolysis Temperature and Particle Size. Environmental Science & Technology, 2013, 47, 821-828.	4.6	295
7	Mechanistic understanding of polychlorinated biphenyls degradation by peroxymonosulfate activated with CuFe2O4 nanoparticles: Key role of superoxide radicals. Chemical Engineering Journal, 2018, 348, 526-534.	6.6	291
8	Mechanism of hydroxyl radical generation from biochar suspensions: Implications to diethyl phthalate degradation. Bioresource Technology, 2015, 176, 210-217.	4.8	284
9	POLSOIL: research on soil pollution in China. Environmental Science and Pollution Research, 2018, 25, 1-3.	2.7	260
10	New insight into the mechanism of peroxymonosulfate activation by sulfur-containing minerals: Role of sulfur conversion in sulfate radical generation. Water Research, 2018, 142, 208-216.	5.3	254
11	Fe 3 O 4 @β-CD nanocomposite as heterogeneous Fenton-like catalyst for enhanced degradation of 4-chlorophenol (4-CP). Applied Catalysis B: Environmental, 2016, 188, 113-122.	10.8	235
12	Efficient transformation of DDTs with Persulfate Activation by Zero-valent Iron Nanoparticles: A Mechanistic Study. Journal of Hazardous Materials, 2016, 316, 232-241.	6.5	181
13	Activation of persulfate with vanadium species for PCBs degradation: A mechanistic study. Applied Catalysis B: Environmental, 2017, 202, 1-11.	10.8	175
14	Humic Acid Facilitates the Transport of ARS-Labeled Hydroxyapatite Nanoparticles in Iron Oxyhydroxide-Coated Sand. Environmental Science & Technology, 2012, 46, 2738-2745.	4.6	172
15	Antagonistic Effects of Humic Acid and Iron Oxyhydroxide Grain-Coating on Biochar Nanoparticle Transport in Saturated Sand. Environmental Science & Technology, 2013, 47, 5154-5161.	4.6	168
16	A scientometric review of biochar research in the past 20Âyears (1998–2018). Biochar, 2019, 1, 23-43.	6.2	160
17	Contribution of alcohol radicals to contaminant degradation in quenching studies of persulfate activation process. Water Research, 2018, 139, 66-73.	5.3	148
18	Electrokinetic remediation of a Cu contaminated red soil by conditioning catholyte pH with different enhancing chemical reagents. Chemosphere, 2004, 56, 265-273.	4.2	143

#	Article	IF	CITATIONS
19	Transformation of polychlorinated biphenyls by persulfate at ambient temperature. Chemosphere, 2013, 90, 1573-1580.	4.2	140
20	Zero-valent iron activated persulfate remediation of polycyclic aromatic hydrocarbon-contaminated soils: An in situ pilot-scale study. Chemical Engineering Journal, 2019, 355, 65-75.	6.6	139
21	Novel and High-Performance Magnetic Carbon Composite Prepared from Waste Hydrochar for Dye Removal. ACS Sustainable Chemistry and Engineering, 2014, 2, 969-977.	3.2	131
22	Electrokinetic remediation of a Cu–Zn contaminated red soil by controlling the voltage and conditioning catholyte pH. Chemosphere, 2005, 61, 519-527.	4.2	122
23	Copper and Zn uptake by radish and pakchoi as affected by application of livestock and poultry manures. Chemosphere, 2005, 59, 167-175.	4.2	121
24	Microbial and enzyme properties of apple orchard soil as affected by long-term application of copper fungicide. Soil Biology and Biochemistry, 2009, 41, 1504-1509.	4.2	121
25	Effect of EDTA, EDDS, NTA and citric acid on electrokinetic remediation of As, Cd, Cr, Cu, Ni, Pb and Zn contaminated dredged marine sediment. Environmental Science and Pollution Research, 2016, 23, 10577-10586.	2.7	119
26	Reductive Hexachloroethane Degradation by S ₂ O ₈ ^{•–} with Thermal Activation of Persulfate under Anaerobic Conditions. Environmental Science & Technology, 2018, 52, 8548-8557.	4.6	117
27	Facilitated transport of Cu with hydroxyapatite nanoparticles in saturated sand: Effects of solution ionic strength and composition. Water Research, 2011, 45, 5905-5915.	5.3	109
28	Role of Hydrochar Properties on the Porosity of Hydrochar-based Porous Carbon for Their Sustainable Application. ACS Sustainable Chemistry and Engineering, 2015, 3, 833-840.	3.2	109
29	Mechanisms of Interaction between Persulfate and Soil Constituents: Activation, Free Radical Formation, Conversion, and Identification. Environmental Science & Technology, 2018, 52, 14352-14361.	4.6	109
30	Effects of exposure pathways on the accumulation and phytotoxicity of silver nanoparticles in soybean and rice. Nanotoxicology, 2017, 11, 699-709.	1.6	107
31	Efficient activation of persulfate decomposition by Cu2FeSnS4 nanomaterial for bisphenol A degradation: Kinetics, performance and mechanism studies. Applied Catalysis B: Environmental, 2019, 253, 278-285.	10.8	107
32	Synergy between Iron and Selenide on FeSe ₂ (111) Surface Driving Peroxymonosulfate Activation for Efficient Degradation of Pollutants. Environmental Science & Technology, 2020, 54, 15489-15498.	4.6	90
33	Transport and re-entrainment of soil colloids in saturated packed column: effects of pH and ionic strength. Journal of Soils and Sediments, 2011, 11, 491-503.	1.5	89
34	A novel peroxymonosulfate activation process by periclase for efficient singlet oxygen-mediated degradation of organic pollutants. Chemical Engineering Journal, 2021, 403, 126445.	6.6	87
35	Production Temperature Effects on the Structure of Hydrochar-Derived Dissolved Organic Matter and Associated Toxicity. Environmental Science & amp; Technology, 2018, 52, 7486-7495.	4.6	86
36	Biofilms and extracellular polymeric substances mediate the transport of graphene oxide nanoparticles in saturated porous media. Journal of Hazardous Materials, 2015, 300, 467-474.	6.5	83

#	Article	IF	CITATIONS
37	Roxarsone binding to soil-derived dissolved organic matter: Insights from multi-spectroscopic techniques. Chemosphere, 2016, 155, 225-233.	4.2	83
38	Effect of different grain sizes of hydroxyapatite on soil heavy metal bioavailability and microbial community composition. Agriculture, Ecosystems and Environment, 2018, 267, 165-173.	2.5	82
39	Biomass Schiff base polymer-derived N-doped porous carbon embedded with CoO nanodots for adsorption and catalytic degradation of chlorophenol by peroxymonosulfate. Journal of Hazardous Materials, 2020, 384, 121345.	6.5	80
40	Enhanced-electrokinetic remediation of copper–pyrene co-contaminated soil with different oxidants and pH control. Chemosphere, 2013, 90, 2326-2331.	4.2	77
41	Effect of iron oxide reductive dissolution on the transformation and immobilization of arsenic in soils: New insights from X-ray photoelectron and X-ray absorption spectroscopy. Journal of Hazardous Materials, 2014, 279, 212-219.	6.5	77
42	Effect of Organic Matter on Sorption of Zn on Soil: Elucidation by Wien Effect Measurements and EXAFS Spectroscopy. Environmental Science & Technology, 2016, 50, 2931-2937.	4.6	77
43	Adsorption of diethyl phthalate ester to clay minerals. Chemosphere, 2015, 119, 690-696.	4.2	75
44	Peroxymonosulfate activation by localized electrons of ZnO oxygen vacancies for contaminant degradation. Chemical Engineering Journal, 2021, 416, 128996.	6.6	73
45	Adsorption and cosorption of cadmium and glyphosate on two soils with different characteristics. Chemosphere, 2004, 57, 1237-1244.	4.2	71
46	Kinetics, intermediates and acute toxicity of arsanilic acid photolysis. Chemosphere, 2014, 107, 274-281.	4.2	71
47	Efficient transformation of DDT by peroxymonosulfate activated with cobalt in aqueous systems: Kinetics, products, and reactive species identification. Chemosphere, 2016, 148, 68-76.	4.2	71
48	Mechanism of metal sulfides accelerating Fe(II)/Fe(III) redox cycling to enhance pollutant degradation by persulfate: Metallic active sites vs. reducing sulfur species. Journal of Hazardous Materials, 2021, 404, 124175.	6.5	71
49	A Mechanistic Understanding of Hydrogen Peroxide Decomposition by Vanadium Minerals for Diethyl Phthalate Degradation. Environmental Science & Technology, 2018, 52, 2178-2185.	4.6	69
50	Transport and retention of silver nanoparticles in soil: Effects of input concentration, particle size and surface coating. Science of the Total Environment, 2019, 648, 102-108.	3.9	68
51	Screening of wheat straw biochars for the remediation of soils polluted with Zn (II) and Cd (II). Journal of Hazardous Materials, 2019, 362, 311-317.	6.5	68
52	Surfactant and oxidant enhanced electrokinetic remediation of a PCBs polluted soil. Separation and Purification Technology, 2014, 123, 106-113.	3.9	66
53	Distribution and Accumulation of Copper and Cadmium in Soil–Rice System as Affected by Soil Amendments. Water, Air, and Soil Pollution, 2009, 196, 29-40.	1.1	65
54	Metagenomic analysis exploring microbial assemblages and functional genes potentially involved in di (2-ethylhexyl) phthalate degradation in soil. Science of the Total Environment, 2020, 715, 137037.	3.9	65

Wang Yimin

#	Article	IF	CITATIONS
55	Hyperexponential and nonmonotonic retention of polyvinylpyrrolidone-coated silver nanoparticles in an Ultisol. Journal of Contaminant Hydrology, 2014, 164, 35-48.	1.6	61
56	Homogenous activation of persulfate by different species of vanadium ions for PCBs degradation. Chemical Engineering Journal, 2017, 323, 84-95.	6.6	61
57	The oxidation and sorption mechanism of Sb on δ-MnO 2. Chemical Engineering Journal, 2018, 342, 429-437.	6.6	61
58	Antimony oxidation and sorption behavior on birnessites with different properties (\hat{l} -MnO2 and) Tj ETQq0 0 0 rg	BT/Qverlo	ock 10 Tf 50 6
59	Pilot-scale electrokinetic treatment of a Cu contaminated red soil. Chemosphere, 2006, 63, 964-971.	4.2	60
60	Surface-modified nanoscale carbon black used as sorbents for Cu(II) and Cd(II). Journal of Hazardous Materials, 2010, 174, 34-39.	6.5	60
61	Ryegrass uptake of soil Cu/Zn induced by EDTA/EDDS together with a vertical direct-current electrical field. Chemosphere, 2007, 67, 1671-1676.	4.2	57
62	Significant contribution of metastable particulate organic matter to natural formation of silver nanoparticles in soils. Nature Communications, 2019, 10, 3775.	5.8	57
63	Investigation on the Physical and Chemical Properties of Hydrochar and Its Derived Pyrolysis Char for Their Potential Application: Influence of Hydrothermal Carbonization Conditions. Energy & Fuels, 2015, 29, 5222-5230.	2.5	56
64	The degradation of diethyl phthalate by reduced smectite clays and dissolved oxygen. Chemical Engineering Journal, 2019, 355, 247-254.	6.6	56
65	Phosphate affects the adsorption of tetracycline on two soils with different characteristics. Geoderma, 2010, 156, 237-242.	2.3	55
66	The transformation and fate of silver nanoparticles in paddy soil: effects of soil organic matter and redox conditions. Environmental Science: Nano, 2017, 4, 919-928.	2.2	55
67	Role of solution chemistry in the retention and release of graphene oxide nanomaterials in uncoated and iron oxide-coated sand. Science of the Total Environment, 2017, 579, 776-785.	3.9	55
68	Environmental and human health risks from metal exposures nearby a Pb-Zn-Ag mine, China. Science of the Total Environment, 2020, 698, 134326.	3.9	55
69	Transport behavior of humic acid-modified nano-hydroxyapatite in saturated packed column: Effects of Cu, ionic strength, and ionic composition. Journal of Colloid and Interface Science, 2011, 360, 398-407.	5.0	54
70	Electrokinetic delivery of persulfate to remediate PCBs polluted soils: Effect of injection spot. Chemosphere, 2014, 117, 410-418.	4.2	54
71	Effect of aqueous Fe(II) on Sb(V) sorption on soil and goethite. Chemosphere, 2016, 147, 44-51.	4.2	53
72	Electrokinetic delivery of persulfate to remediate PCBs polluted soils: Effect of different activation methods. Chemosphere, 2016, 144, 138-147.	4.2	53

#	Article	IF	CITATIONS
73	Speciation and location of arsenic and antimony in rice samples around antimony mining area. Environmental Pollution, 2019, 252, 1439-1447.	3.7	52
74	Laboratory assessment of the mobility of water-dispersed engineered nanoparticles in a red soil (Ultisol). Journal of Hydrology, 2014, 519, 1677-1687.	2.3	51
75	A new insight into the immobilization mechanism of Zn on biochar: the role of anions dissolved from ash. Scientific Reports, 2016, 6, 33630.	1.6	51
76	Comparison of Persulfate Activation and Fenton Reaction in Remediating an Organophosphorus Pesticides-Polluted Soil. Pedosphere, 2017, 27, 465-474.	2.1	48
77	Surface-bound radical control rapid organic contaminant degradation through peroxymonosulfate activation by reduced Fe-bearing smectite clays. Journal of Hazardous Materials, 2020, 389, 121819.	6.5	48
78	Genotypic variation and mechanism in uptake and translocation of perfluorooctanoic acid (PFOA) in lettuce (Lactuca sativa L.) cultivars grown in PFOA-polluted soils. Science of the Total Environment, 2018, 636, 999-1008.	3.9	45
79	Efficient activation of peroxymonosulfate by copper sulfide for diethyl phthalate degradation: Performance, radical generation and mechanism. Science of the Total Environment, 2020, 749, 142387.	3.9	44
80	Transport of ARS-labeled hydroxyapatite nanoparticles in saturated granular media is influenced by surface charge variability even in the presence of humic acid. Journal of Hazardous Materials, 2012, 229-230, 170-176.	6.5	43
81	Mechanistic understanding of reduced AgNP phytotoxicity induced by extracellular polymeric substances. Journal of Hazardous Materials, 2016, 308, 21-28.	6.5	43
82	Mechanism and Implication of the Sorption of Perfluorooctanoic Acid by Varying Soil Size Fractions. Journal of Agricultural and Food Chemistry, 2018, 66, 11569-11579.	2.4	43
83	Application of bioassays to evaluate a copper contaminated soil before and after a pilot-scale electrokinetic remediation. Environmental Pollution, 2009, 157, 410-416.	3.7	42
84	Review of chemical and electrokinetic remediation of PCBs contaminated soils and sediments. Environmental Sciences: Processes and Impacts, 2016, 18, 1140-1156.	1.7	42
85	Demethanation Trend of Hydrochar Induced by Organic Solvent Washing and Its Influence on Hydrochar Activation. Environmental Science & Technology, 2017, 51, 10756-10764.	4.6	42
86	The effects of Fe-bearing smectite clays on OH formation and diethyl phthalate degradation with polyphenols and H2O2. Journal of Hazardous Materials, 2018, 357, 483-490.	6.5	41
87	Facilitated Transport of Copper with Hydroxyapatite Nanoparticles in Saturated Sand. Soil Science Society of America Journal, 2012, 76, 375-388.	1.2	39
88	EDTA-enhanced electrokinetic remediation of aged electroplating contaminated soil assisted by combining dual cation-exchange membranes and circulation methods. Chemosphere, 2020, 243, 125439.	4.2	39
89	Adsorption and desorption of Cu(II), Zn(II), Pb(II), and Cd(II) on the soils amended with nanoscale hydroxyapatite. Environmental Progress and Sustainable Energy, 2010, 29, 233-241.	1.3	38
90	Functional genomic analysis of phthalate acid ester (PAE) catabolism genes in the versatile PAE-mineralising bacterium Rhodococcus sp. 2G. Science of the Total Environment, 2018, 640-641, 646-652.	3.9	38

#	Article	IF	CITATIONS
91	Effects of clay minerals on diethyl phthalate degradation in Fenton reactions. Chemosphere, 2016, 165, 52-58.	4.2	37
92	TiO2 photocatalytic degradation of 4-chlorobiphenyl as affected by solvents and surfactants. Journal of Soils and Sediments, 2012, 12, 376-385.	1.5	36
93	Effects of warming on uptake and translocation of cadmium (Cd) and copper (Cu) in a contaminated soil-rice system under Free Air Temperature Increase (FATI). Chemosphere, 2016, 155, 1-8.	4.2	35
94	Transport of fluorescently labeled hydroxyapatite nanoparticles in saturated granular media at environmentally relevant concentrations of surfactants. Colloids and Surfaces A: Physicochemical and Engineering Aspects, 2014, 457, 58-66.	2.3	34
95	Effects of Fe(II) on Cd(II) immobilization by Mn(III)-rich δ-MnO2. Chemical Engineering Journal, 2018, 353, 167-175.	6.6	34
96	Efficient transformation of DDT with peroxymonosulfate activation by different crystallographic MnO2. Science of the Total Environment, 2021, 759, 142864.	3.9	34
97	Effects of sodium hypochlorite and high pH buffer solution in electrokinetic soil treatment on soil chromium removal and the functional diversity of soil microbial community. Journal of Hazardous Materials, 2007, 142, 111-117.	6.5	33
98	Evidence for the generation of reactive oxygen species from hydroquinone and benzoquinone: Roles in arsenite oxidation. Chemosphere, 2016, 150, 71-78.	4.2	32
99	Biochar decreased the bioavailability of Zn to rice and wheat grains: Insights from microscopic to macroscopic scales. Science of the Total Environment, 2018, 621, 160-167.	3.9	32
100	Evaluating mechanisms for plant-ion (Ca2+, Cu2+, Cd2+ or Ni2+) interactions and their effectiveness on rhizotoxicity. Plant and Soil, 2010, 334, 277-288.	1.8	30
101	Temperature affects cadmium-induced phytotoxicity involved in subcellular cadmium distribution and oxidative stress in wheat roots. Ecotoxicology and Environmental Safety, 2011, 74, 2029-2035.	2.9	30
102	Inhibited transport of graphene oxide nanoparticles in granular quartz sand coated with Bacillus subtilis and Pseudomonas putida biofilms. Chemosphere, 2017, 169, 1-8.	4.2	30
103	Cu2O@β-cyclodextrin as a synergistic catalyst for hydroxyl radical generation and molecular recognitive destruction of aromatic pollutants at neutral pH. Journal of Hazardous Materials, 2018, 357, 109-118.	6.5	30
104	Interactive effects of rice straw biochar and Î ³ -Al2O3 on immobilization of Zn. Journal of Hazardous Materials, 2019, 373, 250-257.	6.5	30
105	Effects of soil properties, nitrogen application, plant phenology, and their interactions on plant uptake of cadmium in wheat. Journal of Hazardous Materials, 2020, 384, 121452.	6.5	30
106	Determination of Trace Perfluoroalkyl Carboxylic Acids in Edible Crop Matrices: Matrix Effect and Method Development. Journal of Agricultural and Food Chemistry, 2017, 65, 8763-8772.	2.4	29
107	Fate of di (2-ethylhexyl) phthalate and its impact on soil bacterial community under aerobic and anaerobic conditions. Chemosphere, 2019, 216, 84-93.	4.2	28
108	A QICAR approach for quantifying binding constants for metal–ligand complexes. Ecotoxicology and Environmental Safety, 2011, 74, 1036-1042.	2.9	27

#	Article	IF	CITATIONS
109	Remediation of polychlorinated biphenyl-contaminated soil by soil washing and subsequent TiO2 photocatalytic degradation. Journal of Soils and Sediments, 2012, 12, 1371-1379.	1.5	27
110	Integration of metal chemical forms and subcellular partitioning to understand metal toxicity in two lettuce (Lactuca sativa L.) cultivars. Plant and Soil, 2014, 384, 201-212.	1.8	27
111	Differential bioaccumulation patterns of nanosized and dissolved silver in a land snail Achatina fulica. Environmental Pollution, 2017, 222, 50-57.	3.7	27
112	Hydrochars and phosphate enhancing the transport of nanoparticle silica in saturated sands. Chemosphere, 2017, 189, 213-223.	4.2	27
113	Migration and decomplexation of metal-chelate complexes causing metal accumulation phenomenon after chelate-enhanced electrokinetic remediation. Journal of Hazardous Materials, 2019, 377, 106-112.	6.5	27
114	Soil geochemistry and digestive solubilization control mercury bioaccumulation in the earthworm Pheretima guillemi. Journal of Hazardous Materials, 2015, 292, 44-51.	6.5	26
115	Extraction and speciation analysis of roxarsone and its metabolites from soils with different physicochemical properties. Journal of Soils and Sediments, 2016, 16, 1557-1568.	1.5	26
116	Transformation of tetracyclines induced by Fe(III)-bearing smectite clays under anoxic dark conditions. Water Research, 2019, 165, 114997.	5.3	26
117	Ion exchange membranes enhance the electrokinetic in situ chemical oxidation of PAH-contaminated soil. Journal of Hazardous Materials, 2020, 382, 121042.	6.5	26
118	Effects of catholyte conditioning on electrokinetic extraction of copper from mine tailings. Environment International, 2005, 31, 885-890.	4.8	25
119	Sorption of roxarsone onto soils with different physicochemical properties. Chemosphere, 2016, 159, 103-112.	4.2	25
120	Cultivar-Dependent Accumulation and Translocation of Perfluorooctanesulfonate among Lettuce (Lactuca sativa L.) Cultivars Grown on Perfluorooctanesulfonate-Contaminated Soil. Journal of Agricultural and Food Chemistry, 2018, 66, 13096-13106.	2.4	25
121	Rapid DDTs degradation by thermally activated persulfate in soil under aerobic and anaerobic conditions: Reductive radicals vs. oxidative radicals. Journal of Hazardous Materials, 2021, 402, 123557.	6.5	25
122	Natural degradation of roxarsone in contrasting soils: Degradation kinetics and transformation products. Science of the Total Environment, 2017, 607-608, 132-140.	3.9	24
123	Effects of molecular weight-fractionated natural organic matter on the phytoavailability of silver nanoparticles. Environmental Science: Nano, 2018, 5, 969-979.	2.2	24
124	Internal distribution of Cd in lettuce and resulting effects on Cd trophic transfer to the snail: Achatina fulica. Chemosphere, 2015, 135, 123-128.	4.2	23
125	High retention of silver sulfide nanoparticles in natural soils. Journal of Hazardous Materials, 2019, 378, 120735.	6.5	23
126	Unraveling the molecular mechanisms of Cd sorption onto MnOx-loaded biochar produced from the Mn-hyperaccumulator Phytolacca americana. Journal of Hazardous Materials, 2022, 423, 127157.	6.5	21

#	Article	IF	CITATIONS
127	Carbon nitride–based cuprous catalysts induced nonradical-led oxidation by peroxydisulfate: Role of cuprous and dissolved oxygen. Chemical Engineering Journal, 2021, 419, 129667.	6.6	20
128	Distribution of free radicals and intermediates during the photodegradation of polychlorinated biphenyls strongly affected byAcosolvents and TiO2 catalyst. Chemosphere, 2016, 144, 628-634.	4.2	18
129	Oral bioaccessibility of silver nanoparticles and ions in natural soils: Importance of soil properties. Environmental Pollution, 2018, 243, 364-373.	3.7	17
130	Long-term dissolution and transformation of ZnO in soils: The roles of soil pH and ZnO particle size. Journal of Hazardous Materials, 2021, 415, 125604.	6.5	17
131	Adsorption Kinetics of Glyphosate and Copper(II) Alone and Together on Two Types of Soils. Soil Science Society of America Journal, 2009, 73, 1995-2001.	1.2	15
132	Citric Acid-Enhanced Electroremediation of Toxic Metal-Contaminated Dredged Sediments: Effect of Open/Closed Orifice Condition, Electric Potential and Surfactant. Pedosphere, 2018, 28, 35-43.	2.1	15
133	Effects of various warming patterns on Cd transfer in soil-rice systems under Free Air Temperature Increase (FATI) conditions. Ecotoxicology and Environmental Safety, 2019, 168, 80-87.	2.9	15
134	Identifying Plant Stress Responses to Roxarsone in Soybean Root Exudates: New Insights from Two-Dimensional Correlation Spectroscopy. Journal of Agricultural and Food Chemistry, 2018, 66, 53-62.	2.4	14
135	Temporal variability in Cu speciation, phytotoxicity, and soil microbial activity of Cu-polluted soils as affected by elevated temperature. Chemosphere, 2018, 194, 285-296.	4.2	14
136	Decarbonylation reaction of saturated and oxidized tar from pyrolysis of low aromaticity biomass boost reduction of hexavalent chromium. Chemical Engineering Journal, 2019, 360, 1042-1050.	6.6	14
137	Mechanism of significant enhancement of VO2-Fenton-like reactions by oxalic acid for diethyl phthalate degradation. Separation and Purification Technology, 2021, 279, 119671.	3.9	14
138	Metabolic response of earthworms (Pheretima guillemi) to silver nanoparticles in sludge-amended soil. Environmental Pollution, 2022, 300, 118954.	3.7	14
139	Nano-α-Fe2O3 enhanced photocatalytic degradation of diethyl phthalate ester by citric Acid/UV (300–400‬nm): A mechanism study. Journal of Photochemistry and Photobiology A: Chemistry, 2018, 360, 78-85.	2.0	13
140	Modeling the interaction and toxicity of Cu-Cd mixture to wheat roots affected by humic acids, in terms of cell membrane surface characteristics. Chemosphere, 2018, 199, 76-83.	4.2	13
141	The overlooked oxidative dissolution of silver sulfide nanoparticles by thermal activation of persulfate: Processes, mechanisms, and influencing factors. Science of the Total Environment, 2021, 760, 144504.	3.9	13
142	Phytotoxicity and uptake of roxarsone by wheat (Triticum aestivum L.) seedlings. Environmental Pollution, 2016, 219, 210-218.	3.7	12
143	Complex Interaction and Adsorption of Glyphosate and Lead in Soil. Soil and Sediment Contamination, 2013, 22, 72-84.	1.1	11
144	Effects of different warming patterns on the translocations of cadmium and copper in a soil–rice seedling system. Environmental Science and Pollution Research, 2015, 22, 15835-15843.	2.7	11

#	Article	IF	CITATIONS
145	Influence of bacterial extracellular polymeric substances on the sorption of Zn on γ-alumina: A combination of FTIR and EXAFS studies. Environmental Pollution, 2017, 220, 997-1004.	3.7	10
146	Deposition and release of carboxylated graphene in saturated porous media: Effect of transient solution chemistry. Chemosphere, 2019, 235, 643-650.	4.2	10
147	Binding and adsorption energy of Cd in soils and its environmental implication for Cd bioavailability. Soil Science Society of America Journal, 2020, 84, 472-482.	1.2	10
148	Calcium and magnesium enhance arsenate rhizotoxicity and uptake in <i>Triticum aestivum</i> . Environmental Toxicology and Chemistry, 2011, 30, 1642-1648.	2.2	9
149	Macroscopic and microscopic investigation of adsorption and precipitation of Zn on Î ³ -alumina in the absence and presence of As. Chemosphere, 2017, 178, 309-316.	4.2	9
150	Free Cu2+ Ions, Cu Fractionation and Microbial Parameters in Soils from Apple Orchards Following Long-Term Application of Copper Fungicides. Pedosphere, 2011, 21, 139-145.	2.1	8
151	Bioavailability of Soil Copper from Different Sources: Integrating Chemical Approaches with Biological Indicators. Pedosphere, 2014, 24, 145-152.	2.1	8
152	Electrokinetic removal of chromium and copper from contaminated soils by lactic acid enhancement in the catholyte. Journal of Environmental Sciences, 2004, 16, 529-32.	3.2	8
153	Efficient activation of peroxymonosulfate by C ₃ N ₅ doped with cobalt for organic contaminant degradation. Environmental Science: Nano, 2022, 9, 2534-2547.	2.2	8
154	Assessment of the Zn–Co mixtures rhizotoxicity under Ca deficiency: Using two conventional mixture models based on the cell membrane surface potential. Chemosphere, 2014, 112, 232-239.	4.2	7
155	Oxidative dissolution of Sb2O3 mediated by surface Mn redox cycling in oxic aquatic systems. Water Research, 2022, 217, 118403.	5.3	7
156	Binding energies of monovalent anions with Fe/Al oxides based on ion activity and suspension Wien effect methods. Journal of Soils and Sediments, 2010, 10, 863-869.	1.5	6
157	Hydroxyl radicals induced mineralization of organic carbon during oxygenation of ferrous mineral-organic matter associations: Adsorption versus coprecipitation. Science of the Total Environment, 2022, 816, 151667.	3.9	6
158	(Fe3+)-UVC-(aliphatic/phenolic carboxyl acids) systems for diethyl phthalate ester degradation: A density functional theory (DFT) and experimental study. Applied Catalysis A: General, 2018, 567, 20-27.	2.2	5
159	Cotransport of Cu with Graphene Oxide in Saturated Porous Media with Varying Degrees of Geochemical Heterogeneity. Water (Switzerland), 2020, 12, 444.	1.2	5
160	Mechanistic insight into sulfite-enhanced diethyl phthalate degradation by hydrogen atom under UV light. Separation and Purification Technology, 2022, 295, 121310.	3.9	5
161	Time-dependent evolution of Zn(II) fractions in soils remediated by wheat straw biochar. Science of the Total Environment, 2020, 717, 137021.	3.9	4
162	Wien effect determination of binding and adsorption energies between positively charged nano-particles and anions. Journal of Soils and Sediments, 2011, 11, 783-788.	1.5	2

#	Article	IF	CITATIONS
163	A novel approach for predicting the uptake and toxicity of metallic and metalloid ions. Plant Signaling and Behavior, 2011, 6, 461-465.	1.2	2
164	Wien effect of Cd/Zn on soil clay fraction and their interaction. Geochemical Transactions, 2018, 19, 5.	1.8	2
165	Greater Bioaccessibility of Silver Nanoparticles in Earthworm than in Soils. Bulletin of Environmental Contamination and Toxicology, 2022, , 1.	1.3	Ο